Sensors and Materials, Vol. 35, No. 9 (2023) 3499–3509
MYU Tokyo

S & M 3407

Light Intensity Required for the Spring Phytoplankton Bloom in the East Sea

Chun Ok Jo,[1] Yunsoo Choi,[2*] Jongseong Ryu,[3]
Su Young Woo,[4] Jae-Myeong Kim,[5] and Wonjong Lee[2]

[1]Oceanscitech Inc., 59-9, Magokjungang-ro, Gangseo-gu, Seoul 07807, Korea
[2]Department of Geoinformatics, University of Seoul, Seoul 02504, Korea
[3]Department of Marine Biotechnology, Anyang University, Incheon 23038, Korea
[4]Department of Environmental Horticulture, University of Seoul, Seoul 02504, Korea
[5]Department of Urban Planning Engineering, Seokyeong University, Seoul 02173, Korea

(Received April 30, 2023; accepted September 5, 2023)

Keywords: satellite remote sensing, spring bloom, chlorophyll-a, mixed layer depth, optimal PAR

Light is one of the primary resources in regulating phytoplankton growth and productivity. Recent satellite observations have started to report optimal light intensities for phytoplankton blooming in various physiological and ecological environments. To investigate the optimal light intensities required for phytoplankton spring bloom development in the East Sea (ES), we constructed a 10-year climatology of the mean photosynthetically available radiation (PAR) in the mixed layer at the onset times of spring blooms using satellite data and *in situ* temperature–depth profiles. The PAR estimates in the southern ES (<40°N) are nearly uniform, with an optimal value of 4.5 ± 2.1 E m^{-2} day^{-1}; this value is comparable to the PAR in the western North Pacific and the North Atlantic, where bloom initiation has been explained by a shallowing of the mixed layer depth and an increase in the light availability. The PAR estimates for the northern ES are also nearly uniform, with an optimal value of 16.0 ± 7.3 E m^{-2} day^{-1}. However, the PAR is about three times larger in the northern ES than in the southern ES. The value of the northern ES is comparable to the PAR estimate in the Southern Ocean, which is known as a high-nutrient and low-chlorophyll region, owing to iron limitation and zooplankton grazing pressures. These distinct regional differences in the PAR estimates indicate that a variety of physiological and ecological conditions can control the onset of spring blooms.

1. Introduction

Light is an essential resource for primary production and phytoplankton growth in the euphotic zone in the ocean. Previous studies based on laboratory culture experiments revealed the maximum phytoplankton growth rate under optimal light intensity.[1–3] These laboratory-derived optimal light intensities have often been used to estimate primary production because of the difficulty in estimating optimal light intensity in the ocean.[1–3] Recently, however, with satellite remote sensing of the ocean color, a few studies have started to show optimal light

*Corresponding author: e-mail: choiys@uos.ac.kr
https://doi.org/10.18494/SAM4489

ISSN 0914-4935

intensities for spring phytoplankton bloom development in the ocean.[1,4–6] For example, Siegel *et al.* found the optimal intensity of photosynthetically available radiation (PAR) required for bloom initiation from 35°N to 75°N in the North Atlantic.[5] Similarly, the spring bloom developed from the Scotian Shelf to Greenland when the mean PAR within the mixed layer reached 15 W m^{-2} day^{-1}.[4,6] Furthermore, Chen *et al.* estimated the optimal sea surface light intensity required for the spring phytoplankton bloom peaks in marginal seas of the Northwest Pacific.[1] These optimal light intensities show characteristics with constant values depending on the sea area, which may vary with physiological and ecological conditions. These aspects indicate that the optimal light intensity can potentially become an indicator of the requirements of spring bloom development.[1]

Spring blooms are the most distinct features of annual phytoplankton productivity cycles in euphotic zones of the ocean. These blooms affect the species composition, abundance, and diversity of marine organisms in a pelagic ecosystem.[7] Changes in carbon export to the deep waters during the blooms are generally expected to affect carbon cycles in the ocean. Because of the importance of marine ecosystems and carbon cycles, many researchers have sought to understand the dynamics of spring blooms and their governing factors.[8,9]

The spring phytoplankton bloom development in the ocean generally occurs with seasonal changes in temperature, light availability, nutrients, and zooplankton grazing pressure.[7] In temperate and subpolar regions of the ocean, the bloom developments have often been explained by seasonal increases in light intensity with the development of water column stratification from winter to spring under conditions of abundant nutrients and low grazing pressure due to deep winter vertical mixing.[8,9] However, depending on the sea area, phytoplankton will be exposed to different conditions of nutrients and zooplankton grazing pressure. If the zooplankton grazing pressure in a sea area is significant, the light intensity required for the blooming can increase to compensate for the losses due to grazing.[5,10] Therefore, the light intensity can be used to diagnose the characteristics of spring bloom dynamics and their governing factors compared with other areas.

The East Sea (ES) is a semi-enclosed marginal sea of the temperate North Pacific. However, the sea has also been considered a miniature ocean owing to its oceanic features, including its basin-scale gyres, mesoscale eddies, subpolar front, deep-water formation, and thermohaline circulation.[11] In the ES, the phytoplankton productivity shows seasonal cycles with spring and fall blooms.[7,12,13] In particular, the phytoplankton spring blooms are characterized as being the most distinct and regular occurrences in the entire ES every year.[7] The spring bloom development has been explained by seasonal increases in light intensity with the development of water column stratification from winter to spring, as in the case of other temperate and subpolar seas.[12,13] The ES is divided by the subpolar front into warm subtropical water and colder subpolar water [Fig. 1(a)]. The wintertime vertical mixing depth is more profound in the subpolar water than in the subtropical water.[14] The nutrient concentrations and zooplankton biomass in the upper layer during spring are higher in the subpolar water than in the subtropical water.[15,16] Therefore, the physiological and ecological environments should be different in these waters, which could provide different optimal light intensities for the bloom developments. Furthermore, it can be assumed that there are distinct regional differences in the characteristics of spring

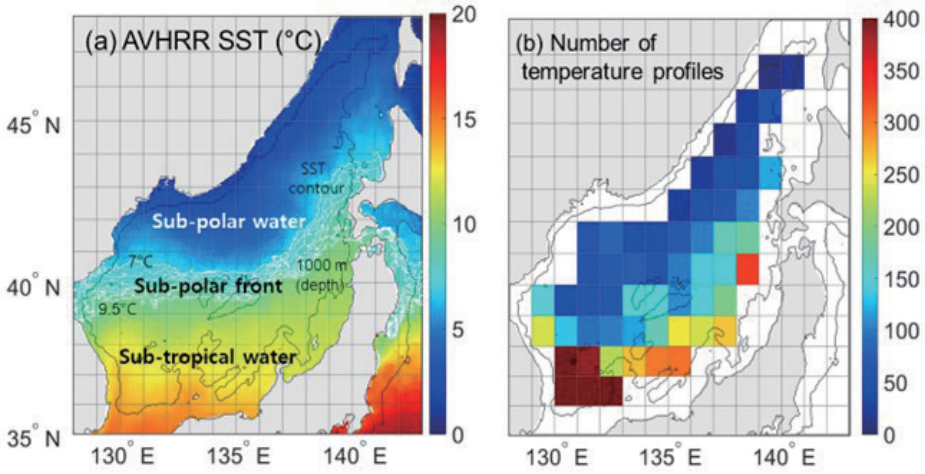

Fig. 1. (Color online) (a) Mean sea surface temperature (°C) during March to May derived from Advanced Very High Resolution Radiometer (AVHRR) from 1998 to 2007 in the ES and (b) number of temperature profiles used for the climatological mixed layer depth (MLD) in a 1° × 1° grid from 1959 to 2007.

bloom dynamics and their governing factors in the ES. However, studies have yet to be conducted on diagnosing the optimal light intensities and characteristics of the bloom dynamics in the ES.

In this study, for the first time, we estimate mean PAR intensities in the mixed layer depth (MLD) at the onset dates of spring blooms to investigate the optimal light intensities required for spring phytoplankton bloom development in the entire ES. We also compared the mean PAR intensities with those in the well-known North Pacific, North Atlantic, and Southern Ocean regarding the control factors of bloom development to understand the characteristics of the bloom dynamics in the ES.

2. Methods

For our analysis of the varying mean PAR intensities in the MLD (I_{MLD}) over seasonal scales, climatological monthly values for chlorophyll-*a* (Chl-*a*) concentrations, PAR, and MLDs are used at a 1° × 1° resolution. MLDs from *in situ* data are not all available in large areas of the ES. They are not in concurrence with Chl-*a* concentration or PAR, which can be derived from continuous satellite ocean color data available for much of the ES. Therefore, climatological MLDs are often estimated using historical data sets of temperature profiles.[5,12] The I_{MLD} was derived from $I_{MLD} = [I_0/(k\text{MLD})]\ (1 - e^{-k\text{MLD}})$, where I_0 is the incident surface PAR and k is the diffuse attenuation coefficient.[17,18] k can be derived from 0.1211 Chl-$a^{0.428}$.[5] Then, the monthly time series of I_{MLD} in each grid was compiled. The uncertainties of the I_{MLD} time series were calculated by error propagation of the uncertainties of the monthly Chl-*a*, MLD, and PAR. The I_{MLD} time series were then used to determine I_{MLD} at the onset date of the spring bloom, from the interpolated I_{MLD} corresponding to the climatological spring bloom onset date.

2.1 Climatological monthly Chl-*a*, PAR, and MLD

For the climatological monthly means of Chl-*a* concentrations and PAR intensities in the study area, we used the monthly composites of Level-3 Standard Mapped Image (SMI) products of the SeaWiFS (Reprocessing, 2010) Chl-*a* concentrations and PAR with a 9 km resolution from 1998 to 2007, which were obtained from the National Aeronautics and Space Administration (NASA), the Goddard Space Flight Center (GSFC), and the Distributed Active Archive Center (DAAC). Mean values of monthly composites in a 1° × 1° grid were calculated each year and compiled to build a 10-year time series of Chl-*a* and PAR with a monthly temporal resolution.[5] Then, climatological monthly means of Chl-*a* concentrations and PAR and their standard deviations (1σ) in each month were determined from the 10-year time series of Chl-*a* and PAR.

Climatological monthly MLDs were derived from individual temperature profiles from 1959 to 2007 obtained from the World Ocean Database 2009 (WOD09) [Fig. 1(b)]. The MLD was defined as the depth at which the temperature differs from that at 10 m depth by 0.2 °C.[14,18,19] Since the MLD estimates in a 1° × 1° grid for a given month generally showed a highly skewed distribution, we adopted the median for the area in a given month to minimize the effect of spatial and temporal outliers. This median deviation was considered to be the uncertainty of the MLD estimate.[19] The median MLDs were compiled to build a climatological monthly MLD time series in the area.

2.2 Estimation of onset date of spring phytoplankton bloom

To obtain a 10-year climatological estimate of the onset date of spring phytoplankton blooms in each 1° × 1° grid, the bloom onset date for each year was determined from the compiled Chl-*a* concentrations described above but with 8-day composites instead of monthly values. Intermittent data gaps in the compiled 8-day Chl-*a* time series were approximated using an asymmetric Gaussian curve ($R^2 > 0.9$).[20] The onsets of spring blooms were defined to be when the fitted Chl-*a* concentration was twice the average taken from the fit in the winter months.[21] For the 10-year climatological estimate of the spring bloom onset time for each grid, the mean bloom onset time and its uncertainty (1σ) were calculated using ten onset times shown in the 10-year Chl-*a* time series.[5] The threshold criteria were previously used to identify the onset dates of spring blooms in the ES.[13,18,21] Yamada *et al.* defined the onset date of a spring bloom as the time when the Chl-*a* exceeds 0.8 mg m^{-3}.[13] Meanwhile, Maúre *et al.* identified the onset date as when the Chl-*a* becomes 5% or 20% higher than the annual median.[18] In our study, the onset dates of spring blooms are essentially the same as those provided by Yamada *et al.* and Maúre *et al.*

3. Results

The spatial distribution of the spring bloom onset dates in the ES reveals a northward propagation of the bloom [Fig. 2(a)]. In the southern ES (< 40°N), the bloom initiates in March, whereas in the northern ES (> 40°N), the bloom initiates in April and early May. These timings

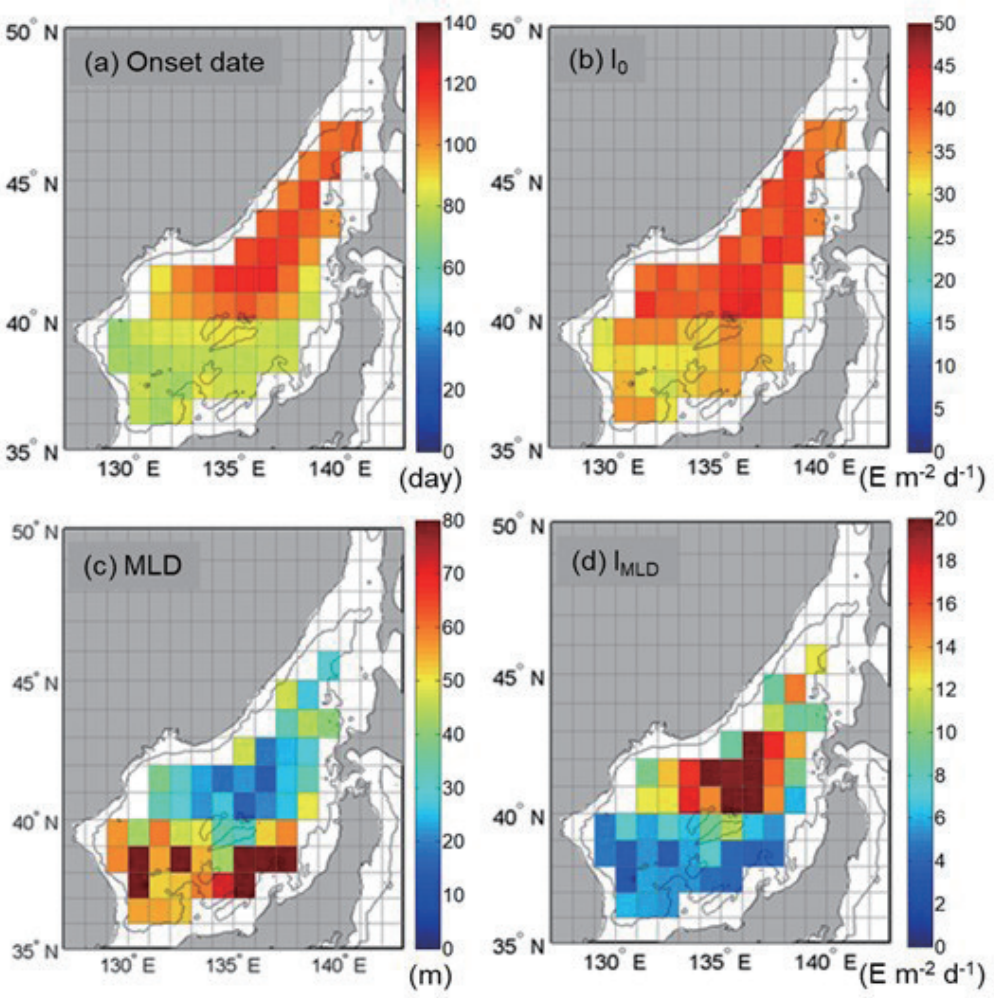

Fig. 2. (Color online) 10-year climatology of (a) the onset date of the spring bloom and (b) I_0, (c) MLD, and (d) IMLD at the spring bloom onset date in the ES for 1° × 1° grids.

are consistent with estimates obtained in other studies.[13,18] The I_0 intensities at the onset dates of spring blooms in the ES vary between 30 and 45 E m^{-2} day^{-1} [Fig. 2(b)]. The MLDs at the bloom onset dates in the southern ES are 60–100 m, about 2–3 times deeper than those at the bloom onset dates in the northern ES [Fig. 2(c)].

The I_{MLD} estimates at the onset dates of the spring bloom show two distinct zones separated by the latitude of 40°N [Fig. 2(d)]. The southern ES is characterized by near-uniform values, with a mean value of 4.5 ± 2.1 E m^{-2} day^{-1}. The values in the northern ES are approximately three times larger, varying between 12 and 22 E m^{-2} day^{-1}. Primarily, the larger values are found in the northeastern ES, where the MLD at the bloom onset date is close to 20 m. Although some outliers exist, the PAR estimates for the northern ES are also nearly uniform, with a mean value of 16.0 ± 7.3 E m^{-2} day^{-1}. Some of the outliers in the estimates may be because the I_{MLD} values are climatological estimates based on the onset date of the spring bloom and the MLD derived from different periods (1998–2007 and 1959–2007, respectively).

4. Discussion

The I_{MLD} estimates in this study exhibit characteristics with constant values in the southern and northern ES [Fig. 2(d)], as shown at the optimal light intensities in other sea areas.[4–6] These constant values indicate that the spring blooms in the southern (36°N to 40°N) and northern (40°N to 46°N) ES could not develop until the light intensities in the mixed layer reached at least about 4.5 ± 2.1 and 16.0 ± 7.3 E m^{-2} day^{-1}, respectively [Fig. 2(d)].

Depending on the sea area, the light intensity required for phytoplankton blooming may vary with physiological and ecological conditions.[5,10] Therefore, the distinct regional differences in I_{MLD} estimates in the ES could suggest that different physiological and ecological conditions could control spring bloom development. To consider these regional differences, we investigate monthly variations in temperature, zooplankton wet weight, and nitrate concentration in MLD in the southern and northern ES (Fig. 3). The data on the zooplankton's wet weight were obtained from Hirota and Hasegawa.[15] The temperature and nitrate concentration in the mixed layer were estimated on the basis of the objectively analyzed (1° grid) climatological monthly data of *in situ* temperature and nitrate measurement data at standard depth levels of the World Ocean Atlas 2009 (WOA09). The temperature and nitrate concentration in the MLD and zooplankton wet weight also showed distinct regional differences between the southern and northern ES (Fig. 3). In the northern ES, phytoplankton experiences much lower temperature, higher nutrient availability, and higher grazing pressure from winter to spring. However, the MLDs between the northern and southern ES do not show distinct regional differences during spring, although the MLDs during winter show significant regional differences.[14]

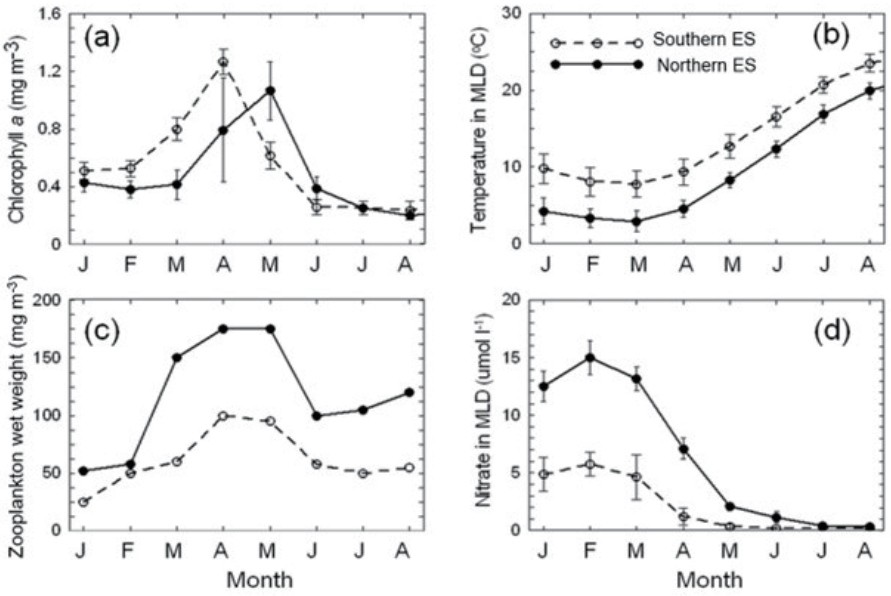

Fig. 3. Climatological monthly variations of the regionally averaged mean of (a) sea surface Chl-*a* concentration, (b) temperature in the mixed layer, (c) zooplankton wet weight, and (d) nitrate concentration in the mixed layer in the southern and northern ES.

Jo *et al*. suggested that phytoplankton in the northern ES could be co-limited by the light availability and iron content owing to severe deep winter mixing.[21] The severe low light intensities can increase the cellular iron demand of phytoplankton and cause iron stress on phytoplankton growth.[21,22] In the northern ES, the I_{MLD} values at the time of bloom initiation are about three times larger than those in the southern ES [Fig. 2(d)]. The co-limitation of phytoplankton by light availability and iron content owing to the deep MLD in winter may result in the later bloom initiation and the larger I_{MLD} in the northern ES.

If the zooplankton grazing pressure is significant during the spring bloom period, then bloom development tends to be delayed or suppressed.[5,10] In the northern ES, the zooplankton biomass generally increases from February and reaches the maximum in April [Fig. 3(c)]. This springtime increase in the zooplankton biomass in the northern ES has been explained by an ontogenetic vertical migration of *Neocalanus* spp. copepods with their 1-yr life cycle.[23] *Neocalanus* spp. spawn below 300 m depth in winter. Young copepodites arrive at the surface layer in March.[24] These newly recruited copepods can rapidly increase their biomass to keep pace with the increase in phytoplankton biomass.[25] Therefore, in the northern ES, the spring bloom may be arrested until I_{MLD} is sufficiently large to overcome the grazing losses by zooplankton, causing the larger I_{MLD} at the bloom initiation time.

We also estimated I_{MLD} at the spring bloom initiation time in the southern Western North Pacific (Southern WNP; 35–39°N, 149–154°E), the northern WNP (Northern WNP; 40–44°N, 149–154°E), the northern North Atlantic (Northern NA; 42–46°N, 35–40°W), and the Southern Ocean (SO; 56–60°S, 45–50°W), where the mechanisms that trigger spring blooms have been studied for decades and have been identified.[5,10,17,26,27] In the selected regions, the I_{MLD} values were estimated like the I_{MLD} estimates in the ES. The I_{MLD} in the southern ES is comparable to that in the Southern WNP, Northern WNP, and Northern NA (Fig. 4). Sverdrup's hypothesis, by which a spring bloom initiation is generally explained by a shallowing of the MLD and an

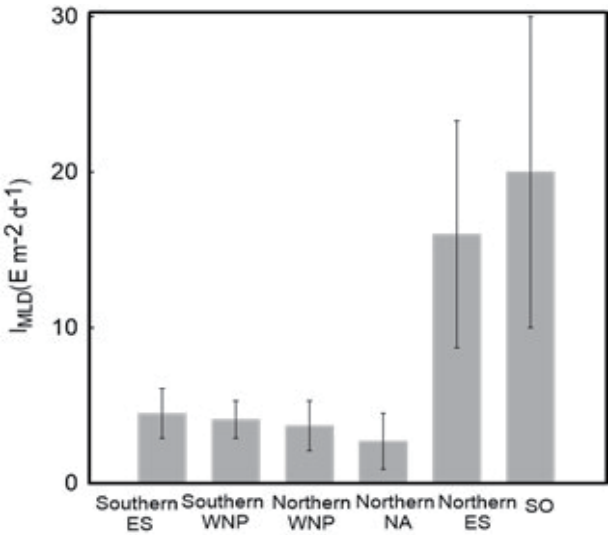

Fig. 4. IMLD estimates at the bloom onset date with corresponding 1σ error bars in the southern and northern ES, Southern WNP, Northern WNP, Northern NA, and SO.

increase in the light availability, has commonly explained the spring bloom in these regions.[5,10,28–30] Meanwhile, I_{MLD} in the northern ES is comparable to that in the SO (Fig. 4). The SO is a high-nutrient and low-chlorophyll (HNLC) region. In this region, phytoplankton blooms are generally suppressed by severe light and iron availability limitations and zooplankton grazing pressure. In the northern ES, phytoplankton may experience not only severe light limitation but also iron limitation and zooplankton grazing pressure before spring bloom initiation, even though the ES is not a HNLC region. This co-limitation may result in more significant I_{MLD} estimates in the northern ES than in the southern ES.

In the ES, the regional differences in spring bloom development and their interannual variations have been generally associated with physical factors controlling light availability, such as MLD, wind speed, eddy, and vertical mixing.[12,13,18] Ecological modeling studies have considered these conditions as the main governing equations and parameters to simulate spatial and temporal variations of spring bloom development in the ES.[16] In our study, however, the distinct regional differences in I_{MLD} estimates and comparisons of these values with those of other ocean regions suggest that physiological and ecological factors should also be considered essential conditions required for the bloom developments in the ES. To clarify this new perspective, quantitative evaluation will be required through field and modeling studies.

5. Conclusions

In this study, we used satellite data and *in situ* temperature profiles to provide a 10-year climatology of the I_{MLD} values at spring bloom initiation in the ES. The I_{MLD} estimates in the southern and northern ES are uniform, with mean values of 4.5 ± 2.1 and 16.0 ± 7.3 E m^{-2} day^{-1}, respectively. These uniform values indicate that the blooms may develop as the light intensities within the mixed layer roughly reach the mean values in both areas. Additionally, the estimated I_{MLD} in the southern ES is comparable to that in the western North Pacific and the North Atlantic, where the improvement of light conditions owing to the shallowing of the MLD has often explained spring bloom development. The estimated I_{MLD} is significantly larger in the northern ES than in the southern ES. The estimated I_{MLD} in the northern ES is comparable to that in the SO, characterized by iron and zooplankton co-limitations. The larger I_{MLD} suggests that phytoplankton in the northern ES may experience more severe physiological or ecological suppression before spring bloom development in the northern ES. Therefore, I_{MLD} can be used to diagnose the effects of the regional characteristics of physiological or ecological factors on the bloom dynamics, although these aspects should be verified. Furthermore, the constant I_{MLD} estimates can be used as a critical parameter of ecological and biogeochemical models to simulate primary productivity and predict spring bloom developments.

The climatological I_{MLD} values were estimated in this study owing to the limitation of MLD data with high spatial and temporal resolutions. If numerical modeling and data assimilation methods provide reliable MLD estimates concurrently with satellite Chl-*a* concentrations, decadal changes in the constant I_{MLD} values in the ES can be analyzed, assuming that the I_{MLD} values increase or decrease in 10-year increments. In this case, it can be expected that phytoplankton will be more severely or less exposed to physiological or ecological limits, resulting in changes in the characteristics of spring bloom dynamics.

Acknowledgments

We thank NASA and the National Oceanic and Atmospheric Administration (NOAA) for providing their satellite Chl-*a* and temperature profile data, respectively. This work was supported by the Basic Study and Interdisciplinary R&D Foundation Fund of the University of Seoul (2019).

References

1 C. Chen, Z. Mao, G. Han, T. Li, Z. Wang, and B. Tao: Ecol. Indic. **72** (2017) 428. https://doi.org/10.1016/j.ecolind.2016.08.044
2 C. Langdon: J. Plankton Res. **9** (1987) 3. https://doi.org/10.1093/plankt/9.3.459
3 T. Platt, C. L. Gallegos, and W. C. Harrison: J. Mar. Res. **38** (1980). https://repositorio.imarpe.gob.pe/bitstream/20.500.12958/1357/1/BOL%20EXTR.%20Investigaci%C3%B3n%20....-18.pdf
4 T. Platt, S. Sathyendranath, G. N. White III, C. Fuentes-Yaco, L. Zhai, E. Devred, and C. Tang: Estuaries Coasts. **33** (2009) 2. https://doi.org/10.1007/s12237-009-9161-0
5 D. A. Siegel, S. C. Doney, and J. A. Yoder: Science **296** (2002) 5568. https://doi.org/10.1126/science.1069174
6 L. Zhai, T. Platt, C. Tang, S. Sathyendranath, and R. H. Walls: ICES J. Mar. Sci. **68** (2011) 4. https://doi.org/10.1093/icesjms/fsq175
7 C. O. Jo, S. Park, Y. H. Kim, K. A. Park, J. J. Park, M. K. Park, S. Li, J. Y. Kim, J. E. Park, J. Y. Kim, and K. R. Kim: J. Mar. Syst. **139** (2014) 288. https://doi.org/10.1016/j.jmarsys.2014.07.004
8 K. Banse and D. C. English: J. Geophys. Res. C: Oceans **99** (1994) C4. https://doi.org/10.1029/93JC02155
9 M. Winder and J. E. Cloern: Phil. Trans. R. Soc. B **365** (2010) 1555. https://doi.org/10.1098/rstb.2010.0125
10 A. Obata, J. Ishizaka, and M. Endoh: J. Geophys. Res. C: Oceans **101** (1996) C9. https://doi.org/10.1029/96JC01734
11 K. Kim, K. R. Kim, D. H. Min, Y. Volkov, J. H. Yoon, and M. Takematsu: Geophys. Res. Lett. **28** (2001) 17. https://doi.org/10.1029/2001GL013078W
12 J. E. Park, K. A. Park, C. K. Kang, and G. Kim: Estuaries Coasts **43** (2020) 630. https://doi.org/10.1007/s12237-019-00671-6
13 K. Yamada, J. Ishizaka, S. Yoo, H. C. Kim, and S. Chiba: Prog. Oceanogr. **61** (2004) 2. https://doi.org/10.1016/j.pocean.2004.06.00
14 S. Lim, C. J. Jang, I. S. Oh, and J. Park: J. Mar. Syst. **96** (2012) 1. https://doi.org/10.1016/j.jmarsys.2012.01.003
15 Y. Hirota and S. Hasegawa: Fish. Oceanogr. **8** (2001) 274. https://doi.org/10.1046/j.1365-2419.1999.00116.x
16 G. Onitsuka and T. Yanagi: J. Oceanogr. **61** (2005) 415. https://doi.org/10.1007/s10872-005-0051-1
17 H. S. Cole, S. Henson, A. P. Martin, and A. Yool: ICES J. Mar. Sci. **72** (2015) 6. https://doi.org/10.1093/icesjms/fsu239
18 E. R. Maúre, J. Ishizaka, C. Sukigara, Y. Mino, H. Aiki, T. Matsuno, H. Tomita, J. I. Goes, and H. R. Gomes: Geophys. Res. Lett. **44** (2017) 21. https://doi.org/10.1002/2017GL074359
19 C. de Boyer Montégut, G. Madec, A. S. Fischer, A. Lazar, and D. Iudicone: J. Geophys. Res. C: Oceans **99** (2004) C12. https://doi.org/10.1029/2004JC002378
20 P. Jönsson and L. Eklundh: Comput. Geosci. **30** (2004) 8. https://doi.org/10.1016/j.cageo.2004.05.006
21 C. O. Jo, J. Y. Lee, K. A. Park, Y. H. Kim, and K. R. Kim: Geophys. Res. Lett. **34** (2007) 5. https://doi.org/10.1029/2006GL027395
22 C. M. Moore, M. M. Mills, A. Milne, R. Langlois, E. P. Achterberg, K. Lochte, R. J. Geider, and J. L. Roche: Global Change Biol. **12** (2006) 4. https://doi.org/10.1111/j.1365-2486.2006.01122.x
23 S. Chiba, Y. Hirota, S. Hasegawa, and T. Saino: Fish. Oceanogr. **14** (2005) 6. https://doi.org/10.1111/j.1365-2419.2005.00355.x
24 A. Limsakula, T. Sainoa, J. I. Goes, and T. Midorikawa: Deep Sea Res. Part II **49** (2002) 24. https://doi.org/10.1016/S0967-0645(02)00208-4
25 T. Kobari, A. Shinada, and A. Tsuda: Prog. Oceanogr. **57** (2003) 3. https://doi.org/10.1016/S0079-6611(03)00102-2
26 L. A. Arteaga, E. Boss, M. J. Behrenfeld, T. K. Westberry, and J. L. Sarmiento: Nat. Commun. **11** (2020) 1. https://doi.org/10.1038/s41467-020-19157-2
27 K. Sasaoka, S. Chiba, and T. Saino: Geophys. Res. Lett. **38** (2011) 15. https://doi.org/10.1029/2011GL048299C
28 H. U. Sverdrup: ICES J. Mar. Sci. **18** (1953) 3. http://www.soest.hawaii.edu/oceanography/courses/OCN626/2010/sverdrup.pdf

29 S. A. Henson, I. Robinson, J. T. Allen, and J. J. Waniek: Deep-Sea Res. I: Oceanogr. Res. Pap. **53** (2006) 10. https://doi.org/10.1016/j.dsr.2006.07.009
30 A. Rumyantseva, S. Henson, A. Martin, A. F. Thompson, G. M. Damerell, J. Kaiser, and K. J. Heywood: Prog. Oceanogr. **178** (2019) 102202. https://doi.org/10.1016/j.pocean.2019.102202

About the Authors

Chun Ok Jo received her Ph.D. degree from the Department of Earth and Environmental Sciences, Seoul National University, in 2013. From 2014 to 2019, she was a postdoctoral researcher at Kyungpook National University. Since 2021, she has been working as a director at Oceanscitech Inc. Her current research interests include marine biogeochemical cycles and remote sensing. (cojoo100@gmail.com)

Yunsoo Choi received his Ph.D. degree from the Department of Civil Engineering, Sungkyunkwan University, in 1992. From 1991 to 2001, he was an associate professor at Hankyong University. Since 2001, he has been a professor at the University of Seoul. His current research interests include geographic information and remote sensing. (choiys@uos.ac.kr)

Jongseong Ryu received his Ph.D. degree from the Department of Earth and Environmental Sciences, Seoul National University, in 2006. From 2010 to 2011, he was a senior researcher at the Korea Institute of Ocean Science and Technology. Since 2011, he has been a professor at Anyang University. His current research interests include marine biology and marine policy. (jsryu90@gmail.com)

Su Young Woo is a professor of environmental horticulture at the University of Seoul. He earned his B.A. and M.A. degrees in 1988 and 1991, respectively, from Seoul National University. He attended the University of Washington College of Forest Resources, Seattle, Washington, and earned his Ph.D. degree in 1996. His current research interests focus on stress ecology, especially the effect of air pollution on vegetation. (wsy@uos.ac.kr)

Jae-Myeong Kim received his Ph.D. degree from the Department of Geoinformatics, University of Seoul, in 2012. From 2013 to 2015, he was a research professor at the University of Seoul. Since 2018, he has been an assistant professor at Seokyeong University His current research interests include geographic information and hydrography. (jm927k@skuniv.ac.kr)

Wonjong Lee received his Ph.D. degree from the Department of Geoinformatics, University of Seoul, in 2023. Since 2023, he has been a researcher at the Institute of Urban Science at the University of Seoul. His current research interests include remote sensing, GNSS, and surveying. (wonjong2@uos.ac.kr)